Hidden order in dielectrics: string condensation, solitons, and the charge-vortex duality

Sergei Khlebnikov

Department of Physics and Astronomy, Purdue University, West Lafayette, IN 47907, USA

Abstract

Description of electrons in a dielectric as solitons of the polarization field holds promise as a method for computer simulations of the dynamics of excited states. For that description to be realistic, the interaction between the solitons (prior to their coupling to electromagnetism) must be short-ranged. We present an analytical study of the mechanism by which this is achieved. It is unusual in that it enables screening of the electrically neutral soliton cores by polarization charges. We also argue that the structure of the solitons allows them to be quantized as either fermions or bosons. At the quantum level, the theory has, in addition to the solitonic electric, elementary magnetic excitations, the quantization of which results in an additional ("topological") contribution to the magnetic susceptibility. In the ground state of a typical dielectric, the effect is weak, but we suggest that it may be enhanced in radiatively excited states of small crystals.

Contents

1 Introduction

Recent years have brought attention to ordered phases of matter in which the order cannot be described within the familiar paradigm of symmetry breaking and which therefore require complementary concepts. By itself, the view that a hidden order, not associated with condensation of any local field, can exists in a condensed-matter system is hardly in doubt: for example, it is well known that a type-II superconductor (in three dimensions) does not have a local order parameter, yet that does not preclude the existence of a continuous phase transition [1]. What is less well established is how common the phenomenon of a hidden order is.

In Ref. [2], we proposed an effective description of an ordinary dielectric solely in terms of the polarization field, with electrons and holes arising as solitons of that field. The existence of unconfined solitons in this model relies on the invariance of the static energy functional with respect to adding closed stings of quantized electric flux. This makes it similar in spirit to the models of string-net condensation, proposed as a description of a non-symmetry-breaking order in Refs. [3, 4]. There is also a similarity with the solitonic theory of baryons of Skyrme [5], although in that case there is symmetry breaking by a local order parameter.

The purpose of the electron-as-soliton picture proposed in Ref. [2] was to enable computer simulations of the excited states containing multiple electrons and holes (which may be possible in the regime where the available phase space is large enough for the solitons representing these particles to be treated classically). Perhaps the most surprising aspect of this picture is that the interaction between the solitons (prior to their coupling to electromagnetism) appears short-ranged. On the one hand, that is of course how it should be if this picture is to have any relevance to real materials. On the other hand, in the limit of an easily polarizable medium, the core of the soliton is practically uncharged and is described by a gauge theory—the lattice electrodynamics of Ref. [6]. The core looks like that of a Dirac monopole [7], a classical solution of that theory [8]. These monopoles are known to have long-range interactions. Making the interaction short-ranged thus requires that the system somehow implements screening of the uncharged cores by polarization charges.

Here, after a review, in Sec. 2, of the soliton properties as seen numerically, we describe,

in Sec. 3, an analytical calculation that allows one to understand the screening mechanism. In particular, we show how the uncharged soliton core sources a polarization cloud with the total charge of unity. The mechanism is distinct from (in a sense, even opposite to) the Debye screening in plasma, wherein a nonzero core charge produces a configuration of the overall charge zero.

We next proceed (Secs. 4–6) to a discussion of quantum effects implied by the solitonic picture. The main outcome of this discussion is a curious version of the charge-vortex duality, one aspect of which is that magnetic vortices (or vortex lines), usually associated with superconductors, persist in dielectrics. Quantization of vorticity is accompanied by a novel ("topological") contribution to the magnetic susceptibility, but we find that in the ground state of a typical dielectric the effect is weak. We suggest that the prospects for its observability may be improved by going to excited states, such as supplied, for instance, by Mie resonances in a small crystals. Finally, we summarize our results in Sec. 7.

2 Solitons and their interactions

The soliton theory of electrons in a dielectric proposed in Ref. [2] employs the usual polarization vector $\boldsymbol{p}$ of macroscopic electrodynamics as its dynamical variable. This vector is defined on a lattice, and its lattice divergence determines the polarization charge density ρ by the usual formula

$$\rho = -\nabla \cdot \boldsymbol{p}\,. \tag{1}$$

In contrast to vectors describing local orders, $\boldsymbol{p}$ has zero expectation value in the ground state and goes to zero at large radii for the soliton solution.

In application to a specific material, the lattice may be expected to correspond to that of the material, but for our present purposes it is sufficient to consider a simple cubic lattice with unit spacing and the primitive vectors oriented along x, y, and z. The polarization vector $\boldsymbol{p} = (p_x, p_y, p_z)$ is defined on the elementary faces (plaquettes) according to the following rule: a plaquette orthogonal to a primitive vector $\boldsymbol{n}$ hosts a single polarization component, $\boldsymbol{n} \cdot \boldsymbol{p}$ (see Fig. 1). We will assume that the components of $\boldsymbol{p}$, as well as the charge density ρ, are measured in units of $e/2\pi$, where e is the electron charge.

In the absence of time-dependence, the theory is characterized by a static energy functional of the form

$$E = \frac{1}{2}\sum_c (\nabla \cdot \boldsymbol{p})^2 + \sum_f V(\boldsymbol{p})\,, \tag{2}$$

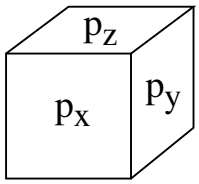

Figure 1: A unit cell of a simple cubic lattice, with each face hosting a single component of the polarization vector $\boldsymbol{p}$.

written for now in arbitrary units. The first sum here is over the unit cells, and the second, involving a potential $V(\boldsymbol{p})$, over the plaquettes. The existence of unconfined solitons relies on the potential $V(\boldsymbol{p})$ being periodic in each of the components of $\boldsymbol{p}$ with period 2π. The way this works is as follows.

Physically, changing $\boldsymbol{p}$ by 2π at a plaquette corresponds to transporting a charge e across that plaquette, as for instance when charges are separated through creation of a particle-hole pair. The periodicity of V reflects quantization of those charges. Due to the first term in (2), the energy of a particle-hole pair is nonzero; however, because of the periodicity of V, it does not grow linearly when the particles are being pulled further apart—and a string of quantized electric flux between them is created. Note that the string lives on the dual lattice, formed by the centers of the units cells of the original. In the present model, electrons and holes are represented by solitons located at the ends of such open strings [2].

The precise form of $V(\boldsymbol{p})$ will not be too important for us here. For definiteness, we choose it, as in [2], as

$$V(\boldsymbol{p}) = \mu^2[1 - \cos(\boldsymbol{n} \cdot \boldsymbol{p})]\,, \tag{3}$$

where $\boldsymbol{n}$ is the unit vector orthogonal to a given plaquette, and μ^2 is a parameter.

Another consequence of the periodicity of $V(\boldsymbol{p})$ is that the static energy is unchanged by adding a closed string of quantized flux. This is what we refer to here as the string condensation. An alternative way to describe it is by way of a lattice analog of the Helmholtz decomposition of $\boldsymbol{p}$. The form of that decomposition is somewhat sensitive to the boundary conditions. A convenient choice is to adopt the Neumann condition for the component of $\boldsymbol{p}$ orthogonal to the boundary and the Dirichlet conditions for the components tangent to it. For example, for those parts of the boundary (b) that face the x direction, we will use discretized versions of

$$\partial_x p_x|_b = 0\,, \qquad p_y|_b = p_z|_b = 0\,. \tag{4}$$

These conditions (together with their counterparts for the y and z directions) ensure that the discrete Laplacian defined on the components of $\boldsymbol{p}$ has the trivial kernel, so we can use the original Helmholtz decomposition,

$$\boldsymbol{p} = \nabla \times \boldsymbol{\psi} + \nabla\chi\,, \tag{5}$$

rather than Hodge's more general version. Here, $\boldsymbol{\psi}$ is a field that lives on the edges of the lattice (one component per edge, in accordance with the edge's direction), and χ is a scalar that lives on the sites of the dual lattice. The lattice curl of $\boldsymbol{\psi}$ is given by the circulation of $\boldsymbol{\psi}$ around a plaquette. The discretization is chosen so that only χ contributes to the divergence in (1):

$$\nabla \cdot \boldsymbol{p} = \nabla^2\chi\,, \tag{6}$$

where ∇^2 is the lattice Laplacian.

Adding an elementary closed string encircling an edge amounts to changing $\boldsymbol{\psi}$ on that edge by 2π. Since this does not affect the value of the energy, one can set up an equivalence relation with respect to such changes [2]. This turns $\boldsymbol{\psi}$ into the gauge field of the compact lattice electrodynamics [6].

The preceding formulas have been written in the continuum notation, but the definitions given make it easy to produce explicit lattice versions. We will do that here for the case of two spatial dimensions (2D), where the physics is much the same but there are fewer indices to keep track of. (Solitons exist also in the one-dimensional version of the theory and, in that case, directly in the continuum, where they are none other than the solitons of the sine-Gordon model. Here, however, our focus is on the 2D and 3D cases.)

In 2D, the field $\boldsymbol{p} = (p_x, p_y)$ has two components defined on the edges of a square lattice with unit spacing, the counterpart of the energy (2) being

$$E = \frac{1}{2}\sum_c (\nabla \cdot \boldsymbol{p})^2 + \sum_{\text{edges}} V(\boldsymbol{p})\,. \tag{7}$$

We again choose $V(\boldsymbol{p})$ in the form (3), except that $\boldsymbol{n}$ is now the unit vector orthogonal to an edge.

The analog of (5) is

$$\boldsymbol{p} = \nabla \times \phi + \nabla\chi\,, \tag{8}$$

where ϕ is a scalar defined on the vertices. In components, $\nabla \times \phi = (\partial_y\phi, -\partial_x\phi)$. The lattice version of (8) is

$$p_x(j,k) \;\; = \;\; \phi_{j,k+1} - \phi_{j,k} + \chi_{j,k} - \chi_{j-1,k}\,, \tag{9}$$

$$p_y(j,k) \;\; = \;\; -(\phi_{j+1,k} - \phi_{j,k}) + \chi_{j,k} - \chi_{j,k-1}\,. \tag{10}$$

Here, the vertices are labeled by a pair of integers (j,k), and we have adopted the convention that a unit cell derives its label from the vertex in its lower left corner. The divergence appearing in (1) becomes

$$(\nabla \cdot \boldsymbol{p})_{j,k} = p_x(j+1,k) - p_x(j,k) + p_y(j,k+1) - p_y(j,k)\,, \tag{11}$$

which together with (9)–(10) can be used to verify (6).

In numerical work, it is convenient to solve the Euler-Lagrange equations corresponding to (2) or (7) directly as they appear in terms of $\boldsymbol{p}$. These equations,

$$-\nabla(\nabla \cdot \boldsymbol{p}) + \partial V/\partial \boldsymbol{p} = 0\,, \tag{12}$$

should be satisfied on each edge (in 2D) or plaquette (in 3D) of the lattice. The soliton solutions can be found numerically by the multidimensional Newton-Raphson method. In Fig. 2, we show results for a single soliton in 2D. The soliton is located at the center of the grid, with the 2π string extending towards the negative x direction. Note that, in addition to p_x, we plot the field $\tilde{p}_x$, which is p_x with the string subtracted: in the continuum notation,

$$p_x(x,y) = \tilde{p}_x(x,y) + 2\pi\delta(y-y_0)\Theta(x_0-x)\,, \tag{13}$$

where Θ is the step function, and (x_0, y_0) is the location of the soliton. The shape of the charge density ρ, obtained by a different method, has appeared in the discussion of multisoliton states in Ref. [2].

The story in 3D is very similar, with one exception. The latter concerns the unstable solutions with multiples $q > 1$ of the elementary charge, by which we mean that they each have a string carrying $2\pi q$ of the electric flux. In 3D, we have found such solutions for all $q \leq 5$. The ones with $q = 4$ and 5 display a curious proliferation of maxima in the density profile, as illustrated for the case $q = 4$ in Fig. 3. There are total of six density maxima in this case (two of these lying off the plane of the plot). That is so even though the components of $\boldsymbol{p}$ themselves do not show any intricate structure, being similar in the overall shape to those of the elementary (stable) soliton. In 2D, on the other hand, we have found an unstable solution (with a single density maximum) for $q = 2$ but none for larger q.

To study the interaction between the solitons, we place a soliton and an anti-soliton at different locations separated by L_s along x and compute the energy as a function of L_s. Subtracting the energy of two well-separated solitons (corresponding here to L_s equal to half

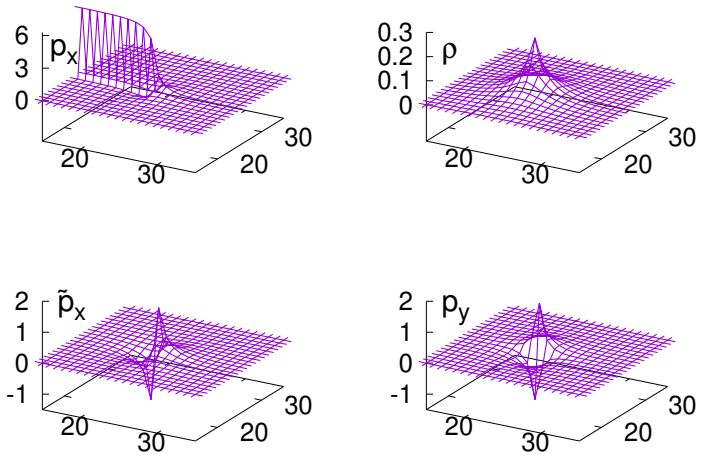

Figure 2: Profiles of the soliton field $\boldsymbol{p}$ and the density $\rho = -\nabla \cdot \boldsymbol{p}$ in two dimensions, computed numerically on a 50×50 grid for the energy functional (7) with $\mu^2 = 0.1$.

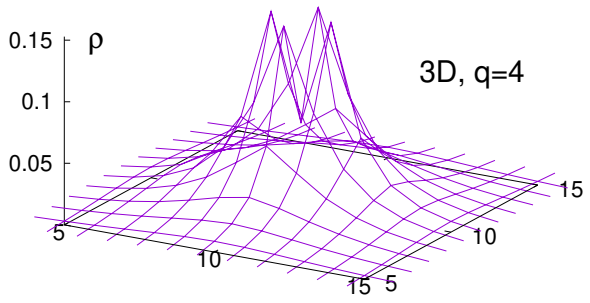

Figure 3: The charge density profile of the unstable solution with charge $q = 4$ in 3D at the (x, y) plane passing through the solution's center, obtained for $\mu^2 = 0.1$ on a 22^3 grid. One can see four maxima of the density; there are two more off the plane, for the total of six.

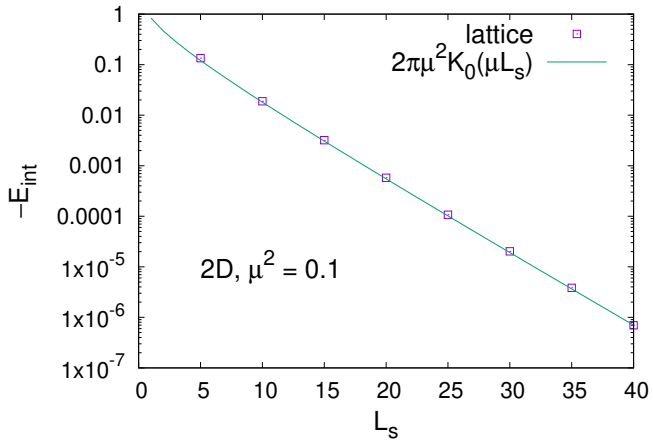

Figure 4: Absolute value of the interaction energy of a soliton-antisoliton pair in 2D as a function of the separation, computed on a 100×50 grid for $\mu^2 = 0.1$. K_0 is the modified Bessel function appearing in the analytical result (27).

the length of the lattice in the x direction), we obtain the interaction energy. A 2D example is shown in Fig. 4. It is important to note that *all* configurations used in this computation are classical solutions: although there is clearly a force between the solitons, as evidenced by the dependence of the energy on L_s, it does not make the configuration unstable, being apparently counteracted by the pinning effect of the lattice. In 3D, the range of accessible interaction energies is not as large, as we only have access to shorter lattices. Still, in that case too, the lattice data clearly show an exponential decay.

3 The screening mechanism

We now describe an analytical method to compute the asymptotics of the fields and the soliton interaction at large distances. The strategy will be to assume (guided, say, by the numerical results of Sec. 2) that the field $\tilde{\boldsymbol{p}}$, which is $\boldsymbol{p}$ with the string subtracted, is small at large distances from the soliton core and argue that it is in fact small there *exponentially*.

As before, we start in two spatial dimensions. Consider first the fields of a single soliton centered at the origin, with the string extending along the negative x axis. We can absorb the string by a redefinition of the field ϕ appearing in (5) into a new field $\tilde{\phi}$. In the continuum notation, we set

$$\phi(x, y) = \arctan(y/x) + \tilde{\phi}(x, y)\,. \tag{14}$$

The field $\tilde{p}_x$, defined by (13) with $x_0 = y_0 = 0$, becomes

$$\tilde{p}_x = \frac{x}{r^2} + \partial_y \tilde{\phi} + \partial_x \chi \equiv b_x + \partial_x \chi \,, \tag{15}$$

where $r^2 = x^2 + y^2$. For uniformity of the notation, we also define $\tilde{p}_y \equiv p_y$, which is

$$\tilde{p}_y = \frac{y}{r^2} - \partial_x \tilde{\phi} + \partial_y \chi \equiv b_y + \partial_y \chi \,. \tag{16}$$

The components $\tilde{p}_x$ and $\tilde{p}_y$ will be assembled into the tilded vector $\tilde{\boldsymbol{p}} = (\tilde{p}_x, \tilde{p}_y)$. In addition, we have defined, as a shorthand, a new field $\boldsymbol{b}$, the components of which can be read off the above.

Replacing $\boldsymbol{p}$ with $\tilde{\boldsymbol{p}}$ does not change the potential (3). Upon that replacement, the energy functional (7), in the continuum notation and on account of Eq. (6), becomes

$$E = \int d^2x \left[\frac{1}{2} (\nabla^2 \chi)^2 + \mu^2 (2 - \cos \tilde{p}_x - \cos \tilde{p}_y) \right] . \tag{17}$$

Consider the contribution to (17) from distances r larger than some $R \gg 1$. Assuming that the magnitude of $\tilde{\boldsymbol{p}}$ decreases to zero at large r, we can, in that contribution, expand the cosines in their arguments. Working to the second order in $\tilde{\boldsymbol{p}}$, we find that contribution to be

$$\Delta E \approx \int_{r>R} d^2x \left\{ \frac{1}{2} (\nabla^2 \chi)^2 + \frac{\mu^2}{2} \left[(\nabla \chi)^2 + 2\boldsymbol{b} \cdot \nabla \chi + \boldsymbol{b}^2 \right] \right\} . \tag{18}$$

If we only want to use this as a basis for obtaining an equation for χ at large r, we can extend the integration in (18) to all radii, but be prepared to encounter a singularity at $r = 0$ (where the expansion in small $\tilde{\boldsymbol{p}}$ does not apply). The singularity appears when we integrate by parts the term with the dot product: this produces $\nabla \cdot \boldsymbol{b}$ which, according to the expressions in (15)–(16), equals $2\pi\delta(\mathbf{r})$. The equation for χ becomes

$$(\nabla^2)^2 \chi - \mu^2 \nabla^2 \chi = 2\pi \mu^2 \delta(\mathbf{r}) \,. \tag{19}$$

The solution, determined up to a constant, is

$$\chi(r) = -K_0(\mu r) - \ln r + \text{const.} \tag{20}$$

The corresponding charge density is $-\nabla^2 \chi = \mu^2 K_0(\mu r)$, and the total charge is

$$Q = -\int \nabla^2 \chi d^2x = 2\pi \,, \tag{21}$$

independently of μ.

Substituting the partial derivatives of the solution (20) into Eqs. (15) and (16), we obtain the following results for the components of the polarization vector:

$$\tilde{p}_x = \frac{x}{r}\mu K_1(\mu r) + \partial_y \tilde{\phi}\,, \tag{22}$$

$$\tilde{p}_y = \frac{y}{r}\mu K_1(\mu r) - \partial_x \tilde{\phi}\,. \tag{23}$$

We can use the same Eq. (18) to obtain the linearized equation for $\tilde{\phi}$ and see if the first terms in (22)–(23) source a nontrivial $\tilde{\phi}$. We find that they do not. So, the pair of Eqs. (22) and (23) with $\tilde{\phi} = 0$ is our final result for the fields at large radii.

The salient point of this result is that the fields decay exponentially: the long-range fields corresponding to the first terms in Eqs. (15) and (16) get precisely canceled by those coming from the logarithm in Eq. (20).

We find this screening effect remarkable, as it is quite distinct from the usual (Debye) screening of an external charge in a linear capacitive environment (for an example of such an environment in 2D, see Ref. [9]). In the latter case, the linearized equation for the polarization vector $\boldsymbol{p}$ (there is no string now, so we do not distinguish between $\boldsymbol{p}$ and $\tilde{\boldsymbol{p}}$) has the form

$$-\nabla(\nabla\cdot\boldsymbol{p}) + \mu^2\boldsymbol{p} = 2\pi\nabla\rho_{ext}\,, \tag{24}$$

where ρ_{ext} is the external charge density. Setting $\boldsymbol{p} = \nabla\chi$ allows one to remove the gradients in (24), to obtain

$$-\nabla^2\chi + \mu^2\chi = 2\pi\rho_{ext}\,. \tag{25}$$

The solution for ρ_{ext} of a unit point charge is $\chi(r) = K_0(\mu r)$, which is clearly different from (20). In particular, the total charge contained in it is zero, while that in (20) is not.

The physical pictures of the two effects are also completely different. This is most easily seen in the limit of a highly polarizable medium, when $\mu \ll 1$. Then, the solution to (25) of the Debye screening case describes a charged core, at $1 \ll r \ll \mu^{-1}$, surrounded by a polarization cloud. In our case, on the other hand, the field (20) is nearly constant at the core, so the core is nearly neutral. The contribution of χ to p_x and p_y is small there, and the fields are essentially those of the vortex of the nonlinear sigma model. The entire charge in this case is contained in a cloud of radius $r \sim \mu^{-1}$, apparently sourced by that neutral core.

The expressions for $\tilde{p}_x$, $\tilde{p}_y$ obtained above can be used to compute the interaction energy of a soliton and an antisoliton separated by a distance $L_s \gg 1$. To the second order in $\tilde{\boldsymbol{p}}$, the interaction energy is

$$E_{int} = \int d^2x \left[(\nabla^2\chi)_1(\nabla^2\chi)_2 + \mu^2\tilde{\boldsymbol{p}}_1\cdot\tilde{\boldsymbol{p}}_2\right]\,, \tag{26}$$

where the subscripts 1 and 2 refer to the soliton and antisoliton, respectively. If $\mu \ll 1$, we can use the continuum expressions (22)–(23) (with $\tilde{\phi} = 0$), since the lattice effects in (26) become negligible. A direct computation then gives

$$E_{int} = -2\pi\mu^2 K_0(\mu L_s)\,. \tag{27}$$

This has been used in Fig. 4 for comparison with the numerical results. For computation of the energy of a single soliton, on the other hand, the continuum approximation can only achieve the logarithmic accuracy (at small μ), as there is a large contribution from $r \sim 1$. For reference, the energy of a single soliton with $\mu^2 = 0.1$, computed numerically, is $E_{sol} = 0.814$.

We wish to stress that Eq. (27) represents interaction of charges through the medium and, as such, applies prior to coupling of the system to electromagnetism. The latter will be described by an *additional* term in the Hamiltonian. This term has the standard structure: for static configurations, it reads

$$H' = -\frac{e}{2\pi}\sum_c \Phi_{el}(\nabla\cdot\boldsymbol{p})\,, \tag{28}$$

where Φ_{el} is the electrostatic potential, and will give rise to the usual Coulomb interaction between the charges. (We will discuss coupling to magnetic fields, which may be important for nonstatic states, in Sec. 5.)

Turning now to three dimensions, we consider a soliton centered at the origin with the string extended along the negative z axis. The counterpart of the decomposition (8) is Eq. (5), and that of (14) is the following expression for the gauge field $\boldsymbol{\psi}$:

$$\boldsymbol{\psi}(\mathbf{r}) = \boldsymbol{\kappa}(\mathbf{r}) + \tilde{\boldsymbol{\psi}}(\mathbf{r})\,, \tag{29}$$

where $\tilde{\boldsymbol{\psi}}$ is the new field (the counterpart of $\tilde{\phi}$ of the 2D case), and $\boldsymbol{\kappa}$ is the vector potential of a magnetic monopole. The monopole vector potential was found by Dirac [7]; in the Cartesian components, it reads

$$\kappa_x = \frac{-y}{4r^2\cos^2(\theta/2)}, \quad \kappa_y = \frac{x}{4r^2\cos^2(\theta/2)}, \quad \kappa_z = 0, \tag{30}$$

where $r = |\mathbf{r}|$, and θ is the polar angle measured from the positive z direction. The polarization vector with the string subtracted is now

$$\tilde{\boldsymbol{p}}(\mathbf{r}) = \frac{\mathbf{r}}{2r^3} + \nabla\times\tilde{\boldsymbol{\psi}} + \nabla\chi\,. \tag{31}$$

The rest of the argument is entirely parallel to that in two dimensions. In particular, the equation for χ is identical to (19) except that the Laplacians and δ-function are now three-dimensional. The solution is

$$\chi(r) = \frac{1}{2r}(1 - e^{-\mu r})\,. \tag{32}$$

We see that the gradient of the long-range (here, $1/r$) part of χ precisely cancels the $\mathbf{r}/r^3$ term in (31). As a result, the fields $\tilde{\boldsymbol{p}}$ decay exponentially.

The interaction between a soliton and an antisoliton at a large separation L_s is given again by Eq. (26) except that the integral is now three-dimensional. As in 2D, we can use in it the continuum expression for χ when $\mu \ll 1$. The result is

$$E_{int} = -\pi\mu^2 \frac{e^{-\mu L_s}}{L_s}\,. \tag{33}$$

For comparison, the energy of a single soliton (which always has to be computed on the lattice) is approximately linear in μ^2 at small μ, $E_{sol} \approx 4.68\mu^2$, but deviates down from this line at larger μ. For $\mu^2 = 0.1$, $E_{sol} = 0.42$.

4 Towards a quantum theory

So far, our considerations have been entirely at the classical level. To proceed to a quantum theory, we must include the static energy E, given by (2) or (7), as a part of a Lagrangian supplying the time dependence. The simplest choice, quadratic in time derivatives, of the Lagrangian in 3D is

$$L = \frac{1}{4\pi K}\sum_f (\partial_t \boldsymbol{p})^2 - \frac{1}{2\pi C}E\,, \tag{34}$$

where the sum is over the elementary faces, and K and C are constant coefficients. In the first term, $\boldsymbol{p}$ refers to the single component that the polarization vector has at each face. Note that $\partial_t \boldsymbol{p}$ is the polarization current density (in units of $e/2\pi$), so K can be interpreted as the intrinsic inverse inductance per unit face, in appropriate units. In the second term, the coefficient $1/2\pi C$ converts the static energy to physical units; C can be interpreted as the intrinsic capacitance per unit cell. In 2D, the sum in (34) has to be replaced by a sum over the edges.

We can immediately identify two types of particle-like excitations in the theory (34). One is the soliton of the preceding sections, whose energy, at the classical level, now depends on both μ^2 and C and may be expected to receive quantum corrections. The other, which

appears at the quantum level, is an optical phonon (a quantum of the polarization wave), with the characteristic energy $E_p = \hbar\sqrt{\alpha K}$, where

$$\alpha \equiv \mu^2/C\,. \tag{35}$$

We expect that an individual soliton can be considered classically when the ratio of these energies, E_p/E_{sol}, is small.

The parameter α can be estimated directly from the dielectric constant ϵ of the material, by looking at the response to a weak constant electric field; the result is [2]

$$\alpha = \frac{2e^2}{a(\epsilon - 1)}\,, \tag{36}$$

where a is the lattice spacing in physical units. The energy E_p can be estimated from the spectrum of the optical phonons. Note that either estimate uses only the small-argument expansion of the cosine potential (3) and, as such, does not rely on the potential's precise form. For example, for silicon, using $a = 5.4\,\text{Å}$ and $\epsilon = 12$ in (36), we find $\alpha = 0.48$ eV. Then, using $E_p = 62$ meV (estimated from the peak in the phonon density of states [10])—and setting $\hbar = 1$, so that K has the dimension of energy—yields $K = 8$ meV.

When there is a finite density of solitons, effects of their quantum statistics can become important. In Fig. 2, we see that, while the charge density is apparently symmetric with respect to exchanging x and y, as well as even with respect to both x and y, the individual polarization components are not. This means that the rotational configuration space of the soliton is the full SO(2) in 2D or SO(3) in 3D. (The lattice pins the orientation of the soliton relative to the lattice directions, just as it pins its position to the center of a unit cell. This pinning, however, is only an energy barrier and does not affect the topology of the configuration space.) Following the well-known argument [11], we then conclude that the solitons can be quantized either as bosons or fermions in 3D, or as anyons in 2D.

5 Quantized vortices in dielectrics

At the quantum level, the theory (34) has yet another type of excitation, one we have not discussed so far. This is the magnetic vortex. It is identified most readily in 2D. Let us use for that the Helmholtz decomposition (8) and proceed to the canonical quantization of the degree of freedom represented by ϕ. The canonical momentum conjugate to ϕ is

$$\Pi = (2\pi K)^{-1}(-\nabla^2)\partial_t\phi\,. \tag{37}$$

Because ϕ_v (on each vertex) is periodic, each Π_v is quantized in integer units.

A boundary condition for ϕ consistent with (4) is $\partial_n \phi|_b = 0$, where ∂_n is the normal derivative. Eq. (37) then implies a constraint (a global equivalent of the Gauss law) $\sum_v \Pi_v = 0$, where the sum is over all the vertices. In practice, however, the correct boundary condition has to be determined case by case and will depend on the properties of the interface that the sample has with other materials. In this section, we adopt the boundary conditions dual to (4), i.e., requiring vanishing of the normal rather than tangential component of $\boldsymbol{p}$. These are consistent with

$$\phi|_b = 0\,. \tag{38}$$

The latter breaks the symmetry $\phi \to \phi + \text{const}$, for which $\sum_v \Pi_v$ is the Noether charge, and makes $\sum_v \Pi_v$ unconstrained. This means that quanta of ϕ can now enter and leave the sample. On the other hand, the normal component of the polarization current at the boundary is now zero. Based on that, we interpret (38) as the boundary condition appropriate at an interface of the sample with vacuum.

Inverting (37) to find the current density carried by ϕ, we see that the eigenstate of Π_v with $\Pi_v = 1$ at some $v = v_0$ and zero everywhere else describes a vortex pattern of current around v_0. We will refer to these vortices as magnetic, to distinguish them from the vortices at the cores of the electrically charged solitons considered in the preceding sections.

The kinetic term for ϕ in the Hamiltonian is

$$H_{kin} = \pi K \sum_v \Pi (-\nabla^2)^{-1} \Pi\,. \tag{39}$$

To understand its role, it is useful to consider first the limit when K is the largest energy scale in the problem, namely, $K \gg \alpha$. This is not the case in conventional dielectrics but can occur in a synthetic material—an array of Josephson junctions (JJs). (For an experimental study of the phase diagram of such an array, see Ref. [12].) We associate $K \ll \alpha$ with the insulating phase, and $K \gg \alpha$ with the superconducting (SC) phase of the array. In the SC phase, Eq. (39) is the leading term in the Hamiltonian of ϕ, so the eigenstates of Π are also approximate eigenstates of the Hamiltonian. Eq. (39) then describes a logarithmic interaction between the magnetic vortices. This makes it clear that the vortices in question are none other than the usual vortices of the superconductor, with the parameter K being proportional to the Josephson energy.

As one moves across the phase boundary to the insulating phase of the array, one can no longer rely solely on H_{kin}, as the second term in (34) becomes important. In this case,

one may prefer to think of charges as solitons of the theory identical to the one described in Sec. 2. (Since the natural unit of polarization in a superconductor is $2e/2\pi$, one may have to interpret the solitons as Cooper pairs and quantize them as bosons.) On the other hand, the magnetic vortices can no longer be described semiclassically. We should use instead the fully quantum definition, with the addition of a vortex at site v_0 defined as the action of any operator $\mathcal{O}(v_0)$ such that

$$[\Pi_v, \mathcal{O}(v_0)] = \delta_{v,v_0}\mathcal{O}(v_0)\,, \tag{40}$$

where the square brackets denote a commutator.

Another way to arrive at the interpretation of the eigenstates of Π as magnetic vortices is to consider interaction of our system with an external vector potential $\mathbf{A}$. It is given, in parallel to (28), by the Lagrangian

$$L'' = \frac{e}{2\pi c}\sum_{\text{edges}} \mathbf{A}\cdot\partial_t \boldsymbol{p}\,, \tag{41}$$

where c is the speed of light in vacuum. Addition of (41) changes the canonical momentum of ϕ from (37) to

$$\Pi = (2\pi K)^{-1}(-\nabla^2)\partial_t\phi + (e/2\pi c)\Phi\,, \tag{42}$$

where $\Phi = (\nabla\times\mathbf{A})_\perp$ is the perpendicular magnetic flux through a unit cell of the dual lattice, in units where the lattice spacing is set to one. This leads to the replacement $\Pi \to \Pi - (e/2\pi c)\Phi$ in the kinetic term (39), which shows that a state with a nonzero expectation value of Π_v carries a density of the magnetic moment.

In 3D, the counterpart of ϕ is the gauge field $\boldsymbol{\psi}$ of (5). Instead of the global symmetry $\phi\to\phi+\text{const}$, we now have the gauge symmetry $\boldsymbol{\psi}\to\boldsymbol{\psi}+\nabla f$. Accordingly, the constraint is now the usual Gauss law $\nabla\cdot\boldsymbol{\Pi}=0$, where $\boldsymbol{\Pi}$ is the momentum conjugate to $\boldsymbol{\psi}$; just as $\boldsymbol{\psi}$ itself, it lives on the lattice edges. As usual in lattice gauge theories, the Gauss law represents conservation of flux at the vertices [13], so the magnetic vortices become vortex lines.

6 Prospects for observability

The existence of quantized magnetic vortices in a dielectric is a somewhat unusual prediction of the present theory, so it is natural to ask what may be its observable consequences. In this section, we will be dealing with purely magnetic excitations, so we now set the charge field

χ to zero. Consistency of this requires that $\nabla \cdot \boldsymbol{p} = 0$; under this condition, the equations of motion for (34) split into separate equations for the individual $\boldsymbol{p}$ on each plaquette.

In the case of a time-independent magnetic field, the interaction Lagrangian (41) is "topological," in the sense that it does not contribute to the equations of motion and so is invisible at the classical level. At the quantum level, however, it can contribute a phase factor to a transition amplitude. In particular, when continued to the Euclidean (imaginary) time via $t = -i\tau$, the present theory has a classical solution (instanton), for which a component of $\boldsymbol{\psi}(\tau)$, say, $\psi_z(\tau)$ changes from zero to 2π at a single edge, while remaining zero at all the other edges. In view of the relation $\boldsymbol{p} = \nabla \times \boldsymbol{\psi}$, this corresponds to a circular polarization current, transporting (in the Euclidean time) a unit charge around that edge. The current is nonzero only at the four plaquettes that meet at the edge. The Euclidean action of such a configuration, in a uniform magnetic field that has a component $B_z \equiv B$ in the z direction, is

$$S_E = \frac{1}{2\pi} \int d\tau \left\{ \frac{4}{2K} (\partial_\tau \psi_z)^2 + 4\alpha(1 - \cos\psi_z) - \frac{ie\Phi}{c} \partial_\tau \psi_z \right\} , \tag{43}$$

where $\Phi = Ba^2$ is the magnetic flux through an elementary square. In this expression for Φ, we have restored the lattice spacing a, which is now in physical units.

One may note that the action (43) is formally identical to that of a short superconducting wire written in terms of the variable—the dipole moment—dual to the difference between the order parameter phases at the wire's ends, with the case $\alpha \gg K$, of interest to us here, corresponding to the regime where the wire is nearly insulating [14, 15]. In the present system, the equivalent "wire" is formed by the current circulating around a lattice edge.

In the transition amplitude, each instanton contributes a factor $e^{ie\Phi/c}$, and each anti-instanton a factor $e^{-ie\Phi/c}$. This results in the ground-state energy, $E_0(B)$, becoming B-dependent. In the approximation where the instantons form a dilute gas,

$$E_0(B) = -2\bar{n} N_{tot} \cos(eBa^2/c) + \text{const} , \tag{44}$$

when $\bar{n}$ is the instanton density (the average number of instantons per edge per unit time), and N_{tot} is the total number of edges in the z direction. Differentiating (44) twice with respect to B at $B = 0$ and dividing by $N_{tot} a^3$ produces the volume magnetic susceptibility

$$\chi_{vol} = -\frac{2\bar{n}e^2 a}{c^2} = -7.4 \times 10^{-6} (\bar{n}/\text{eV})(a/\text{Å}) \tag{45}$$

(in CGS units).

In the ground state of a typical dielectric (for which $\alpha \gg K$), the contribution (45) to the magnetic susceptibility is exponentially suppressed. Indeed, the profile of the instanton of

the theory (43) is that of the well-known soliton of the sine-Gordon model, with the soliton energy

$$S_0 = \frac{16}{\pi}(\alpha/K)^{1/2} \tag{46}$$

now playing the role of the real part of the instanton action. For the values of the parameters listed in Sec. 4, the suppression of $\bar{n}$, due to the semiclassical factor e^{-S_0}, is very strong. One should keep in mind that, unlike the estimates in Sec. 4, the value of the instanton action relies on the precise shape of the cosine potential. Since the latter is only a model chosen for illustration, the value (46) may in practice not be accurate enough. Still, a comparably strong suppression should be expected also for a more realistic potential, given that the susceptibility in question is ultimately a result of electrons tunneling along a path connecting different atoms.

On the other hand, it is known that tunneling amplitudes often grow rapidly (exponentially) with the amount of excitation available in the initial state. To prevent that initial excitation from dispersing, it appears advantageous to consider, instead of a large uniform sample, an array of small dielectrics (nanocrystals). Enhancement of the magnetic response of small dielectrics is well known in optics (for a review, see Ref. [16]), where it is described as a resonance of Mie's classical scattering theory. It would be interesting to see if the topological part (45) of the dc susceptibility is sufficiently enhanced at such a resonance (of the crystal with external radiation) to allow for its experimental measurement.

One may notice that the use of small linear dimensions of a sample for control of the magnetic response in this proposal has some similarity with the use of a small superconductor—a Cooper-pair box (CPB) [17, 18]—for control of the electric charge. We should remark, though, that the exponentially suppressed susceptibility found here for the ground state means that the latter corresponds to a CPB in the regime of *weak* charge quantization, i.e., the transmon regime [19].

7 Conclusion

We thus arrive at a curiously complete instance of the charge-vortex duality, with a near perfect symmetry between the electric and magnetic charges. Each can be considered, under suitable conditions, either as elementary or as solitonic. This duality is characteristic of theories that obey a certain periodicity requirement—namely, the invariance of the static energy with respect to adding closed strings of integer electric flux. In the present paper, we

have focused on the consequences of this duality for dielectrics, where two effects stand out.

One is the existence of solitonic electrically charged excitations, with a charge density possibly extending over several lattice volumes [2]. Here, we have developed an analytical understanding of the mechanism by which the total electric charge of unity is accumulated over a finite distance, starting from an uncharged core. (This is opposite to the usual Debye screening, which starts with a charged particle and results in an object of the overall charge zero.) We have also obtained analytical results for the interaction between the solitons, confirming that it is short-ranged (prior to their coupling to electromagnetism), which is essential for models of this type to be viable as the basis for classical simulations of the carrier dynamics. We have also argued that the structure of the solitons allows them to be quantized as either fermions or bosons (or anyons in 2D).

The second effect is the existence of quantized magnetic vortices associated with circular polarization currents. We have seen that, in the ground state of a typical dielectric, the sensitivity to the quantization of vorticity is exponentially small. A possible route to enhancing it may be access to an excited state of a small crystal via a Mie resonance.

Finally, while experimental discovery of either effect in a conventional dielectric would be most interesting, one may also consider searching for them in a synthetic insulator, formed by an array of Josephson junctions. In that case, one may be able adjust the parameters to one's advantage.

References

[1] C. Dasgupta and B. I. Halperin, "Phase Transition in a Lattice Model of Superconductivity," Phys. Rev. Lett. **47**, 1556 (1981).

[2] S. Khlebnikov, "Electron as soliton: Nonlinear theory of dielectric polarization," arXiv:0710.0414.

[3] M. A. Levin and X.-G. Wen. "String-net condensation: A physical mechanism for topological phases," Phys. Rev. B **71**, 045110 (2005).

[4] X.-G. Wen, "An introduction to quantum order, string-net condensation, and emergence of light and fermions," Ann. Phys. **316**, 1 (2005).

[5] T. H. R. Skyrme, "A non-linear field theory," Proc. R. Soc. A **260**, 127 (1961).

[6] K. G. Wilson, "Confinement of quarks," Phys. Rev. D **10**, 2445 (1974).

[7] P. A. M. Dirac, "Quantised Singularities in the Electromagnetic Field," Proc. R. Soc. A **133**, 60 (1931).

[8] A. M. Polyakov, "Compact gauge fields and the infrared catastrophe," Phys. Lett. **59B**, 82 (1975).

[9] J. E. Mooij, B. J. van Wees, L. J. Geerligs, M. Peters, R. Fazio, and G. Schön, "Unbinding of Charge-Anticharge Pairs in Two-Dimensional Arrays of Small Tunnel Junctions," Phys. Rev. Lett. **65**, 645 (1990).

[10] S. Wei and M. Y. Chou, "Phonon dispersions of silicon and germanium from first-principles calculations," Phys. Rev. B **50**, 2221 (1994).

[11] D. Finkelstein and J. Rubinstein, "Connection between Spin, Statistics, and Kinks," J. Math. Phys. **9**, 1762 (1968).

[12] C. G. L. Bøttcher, F. Nichele, M. Kjaergaard, H. J. Suominen, J. Shabani, C. J. Palmstrøm, and C. M. Marcus, "Superconducting, insulating and anomalous metallic regimes in a gated two-dimensional semiconductor-superconductor array," Nature Phys. **14**, 1138 (2018).

[13] J. Kogut and L. Susskind, "Hamiltonian formulation of Wilson's lattice gauge theories," Phys. Rev. D **11**, 395 (1975).

[14] J. E. Mooij and Yu. V. Nazarov, "Superconducting nanowires as quantum phase-slip junctions," Nature Phys. **2**, 169 (2006).

[15] S. Khlebnikov, "Quantum mechanics of superconducting nanowires," Phys. Rev. B **78**, 014512 (2008).

[16] S. Jahani and Z. Jacob, "All-dielectric metamaterials," Nature Nanotech. **11**, 23 (2016).

[17] M. Büttiker, "Zero-current persistent potential drop across small-capacitance Josephson junctions," Phys. Rev. B **36**, 3548 (1987).

[18] V. Bouchiat, D. Vion, P. Joyez, D. Esteve, and M. H. Devoret, "Quantum Coherence with a Single Cooper Pair," Physica Scripta **T76**, 165 (1998).

[19] J. Koch *et al.*, "Charge-insensitive qubit design derived from the Cooper pair box," Phys. Rev. A **76**, 042319 (2007).